

MHD Calculation of halo currents and vessel forces in NSTX VDEs

J.A. Breslau¹, H.R. Strauss², R. Paccagnella³, S.P. Gerhardt¹

¹Princeton Plasma Physics Laboratory, Princeton, NJ

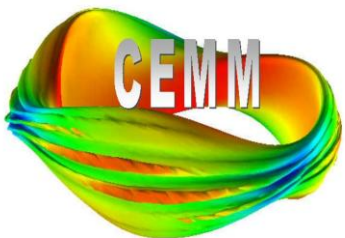
²HRS Fusion LLC, West Orange, NJ

³Consorzio RFX, Padua, Italy

APS-DPP Conference

Providence, RI

October 31, 2012



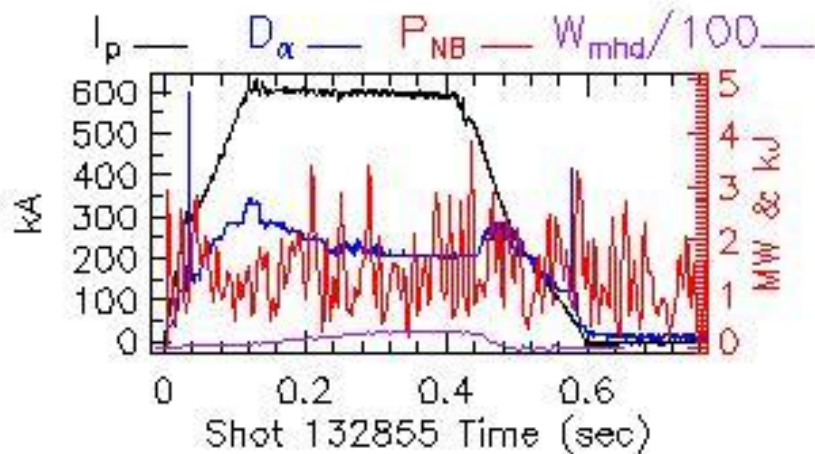
Motivation

- A significant fraction of tokamak discharges at fusion-relevant parameters terminate in disruptions.
- As experiments are scaled up, the stored energy becomes higher, and the potential structural damage due to each disruption increases.
- Accurate quantitative prediction of the distributions of transient currents and attendant forces in conducting structures surrounding a disrupting ITER plasma is vital so that these structures can be designed to survive them.
- M3D, a 3D nonlinear MHD code with resistive wall boundary conditions, is an appropriate tool for calculating currents and forces due to disruptions, but must first be validated against data from experiments such as NSTX, in which they are not catastrophic.
- VDEs are investigated first because they allow the plasma to reach the wall with most of its current, causing the greatest potential damage.

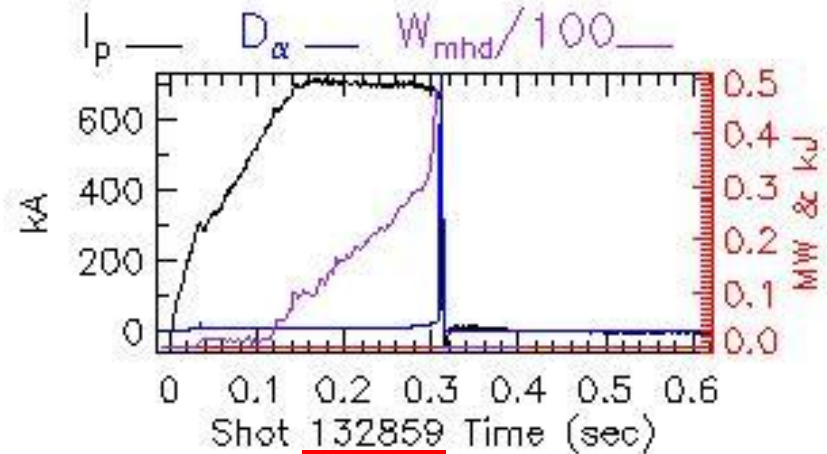
NSTX XP833 (2010):

Halo current dependencies on I_p/q_{95} , vertical velocity, and halo resistance

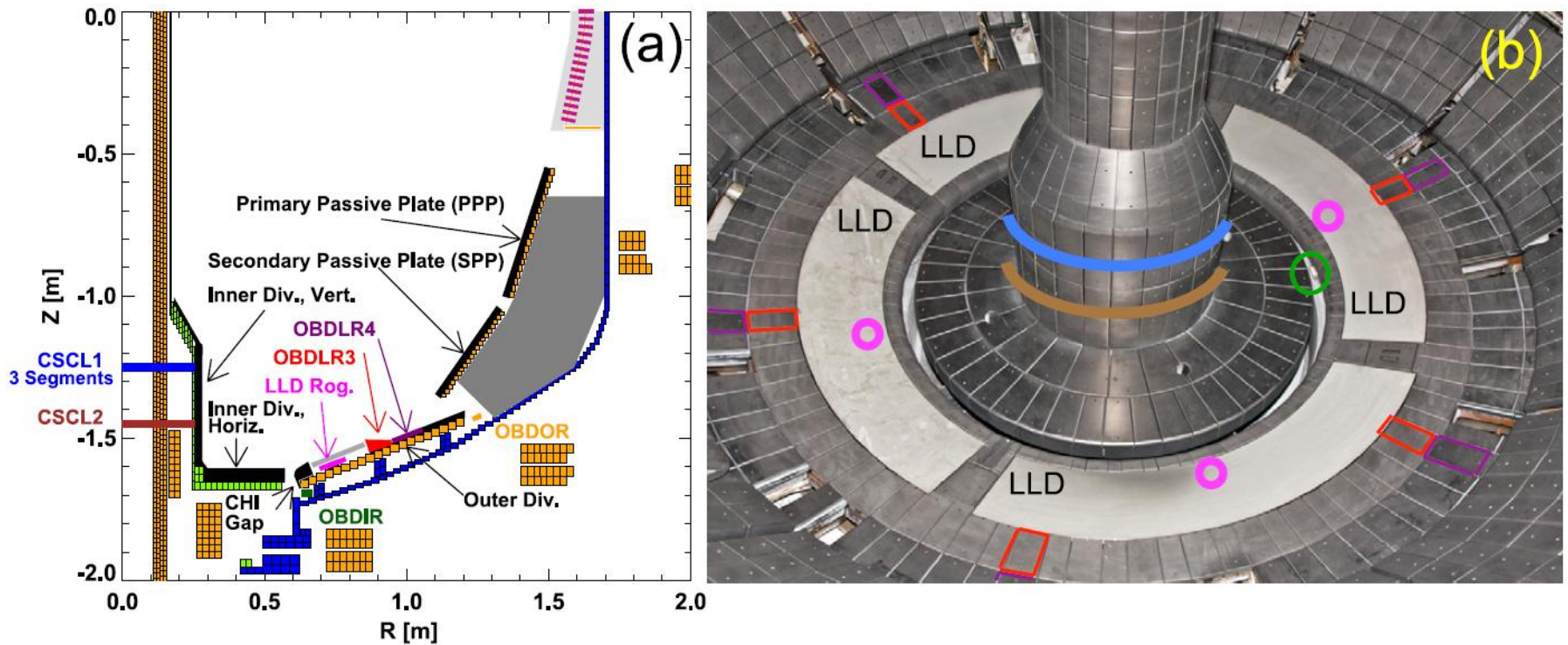
Reference shot without forced disruption drive, based on 129416:



Shot 132859, with deliberately misadjusted vertical field control, terminates in VDE:



Layout of NSTX halo current diagnostics



Halo current is inferred from transient TF measurements under several divertor tiles and plates at about six toroidal locations. Transient vessel forces are not measured.

Typical Experimental Observations (downward-going VDE; not 132859)

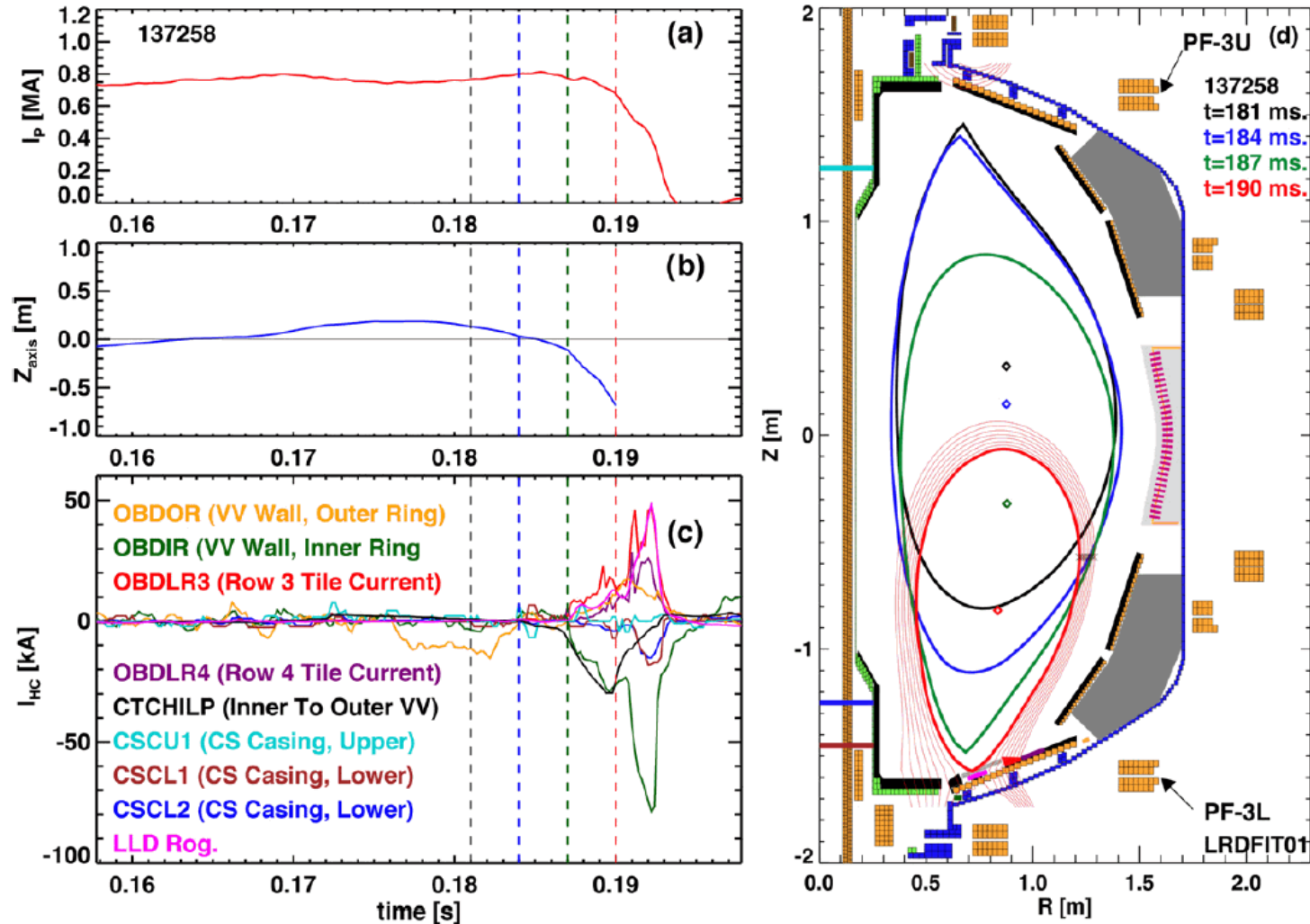


Figure reproduced from S.P. Gerhardt, J. Menard, S. Sabbagh and F. Scotti, *Nucl. Fusion* **52** (2012).

The M3D Code

M3D (multi-level 3D) is a parallel 3D nonlinear extended MHD code in toroidal geometry maintained by a multi-institutional collaboration.

- Physics models include ideal and resistive MHD; two-fluid with just ω^* or ω^* and Hall terms; or hybrid with kinetic hot ions or kinetic bulk ions and fluid electrons.
- Uses linear, 2nd, or 3rd-order finite elements in-plane.
- Uses 4th-order finite differences between planes or pseudo-spectral derivatives.
- Partially implicit treatment allows efficient advance over dissipative and fast wave time scales but requires small time steps relative to τ_A .
- Linear operation: full nonlinear + filtering, active equilibrium maintenance to find fastest-growing toroidal eigenmodes.
- Nonlinear operation: all components of all quantities evolve nonlinearly.
- The PETSc library is used for parallelization and linear solves with Krylov methods.

Extended MHD Equations

$$\frac{\partial \rho}{\partial t} + \nabla \cdot (\rho \mathbf{v}_i) = 0$$

$$\rho \left[\frac{\partial \mathbf{v}}{\partial t} + \mathbf{v} \cdot \nabla \mathbf{v} + (\mathbf{v}_i^* \cdot \nabla) \mathbf{v}_\perp \right] = -\nabla p + \mathbf{J} \times \mathbf{B} + \mu \nabla^2 \mathbf{v}$$

$$\mathbf{E} + \mathbf{v} \times \mathbf{B} = \eta \mathbf{J} - \frac{\nabla_\parallel p_e}{ne}$$

$$\frac{\partial \mathbf{B}}{\partial t} = -\nabla \times \mathbf{E}$$

$$\mathbf{J} = \nabla \times \mathbf{B}$$

$$\frac{\partial p}{\partial t} + \mathbf{v} \cdot \nabla p = -\gamma p \nabla \cdot \mathbf{v} + \nabla \cdot n \chi_\perp \nabla \left(\frac{p}{\rho} \right) - \mathbf{v}_i^* \cdot \nabla p - \gamma p \nabla \cdot \mathbf{v}_i^* + \frac{\mathbf{J} \cdot \nabla p_e}{ne} + \gamma p_e \mathbf{J} \cdot \nabla \left(\frac{1}{ne} \right)$$

$$\frac{\partial p_e}{\partial t} + \mathbf{v} \cdot \nabla p_e = -\gamma p_e \nabla \cdot \mathbf{v} + \nabla \cdot n \chi_{\perp e} \nabla \left(\frac{p_e}{\rho} \right) + \frac{\mathbf{J}_\parallel \cdot \nabla p_e}{ne} - \gamma p_e \nabla \cdot \left(\mathbf{v}_e^* - \frac{\mathbf{J}_\parallel}{ne} \right)$$

where

$$\mathbf{v}_e^* \equiv -\frac{\mathbf{B} \times \nabla p_e}{neB^2}, \quad \mathbf{v}_i^* \equiv \mathbf{v}_e^* + \frac{\mathbf{J}_\perp}{ne},$$

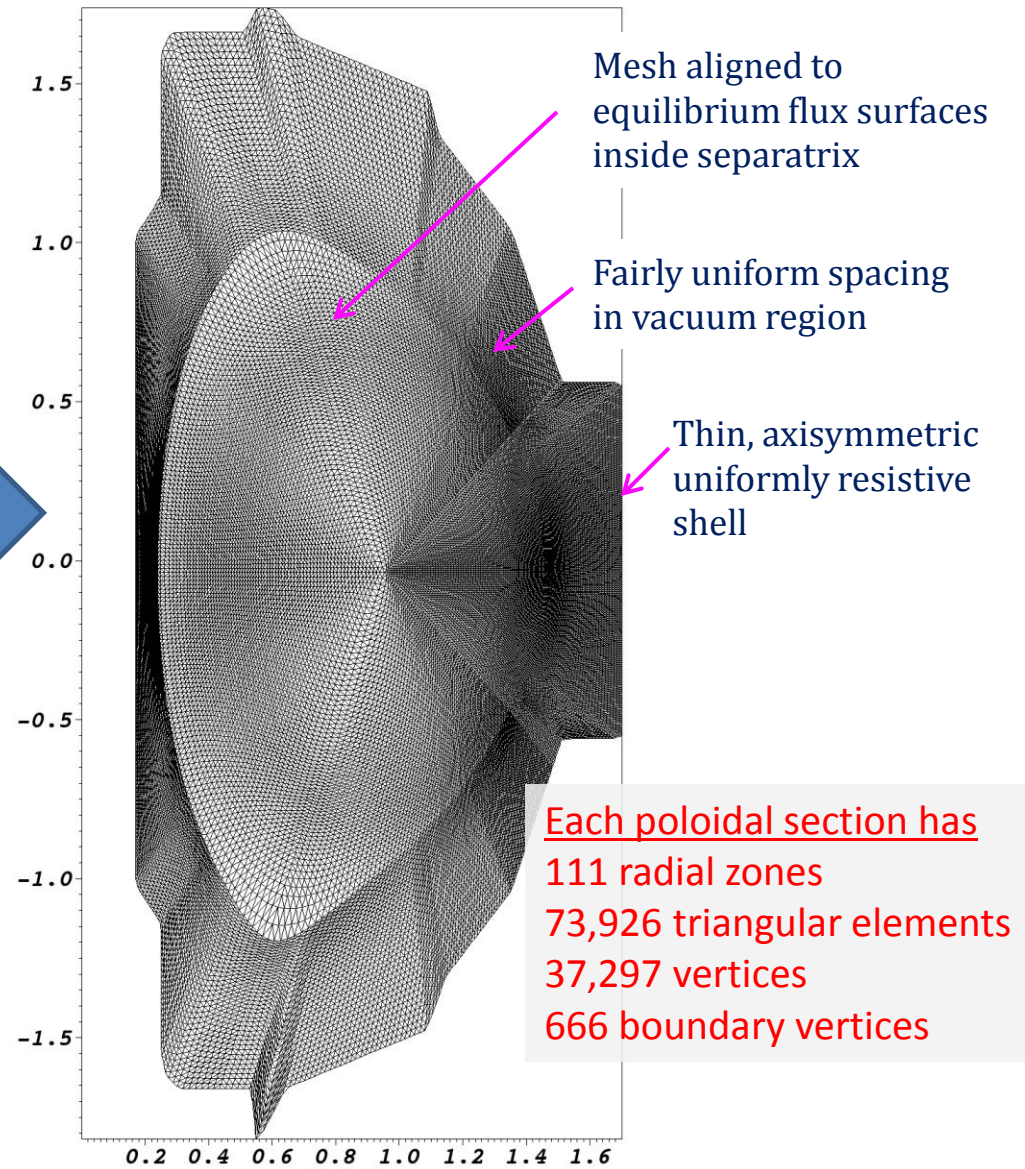
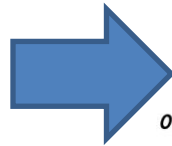
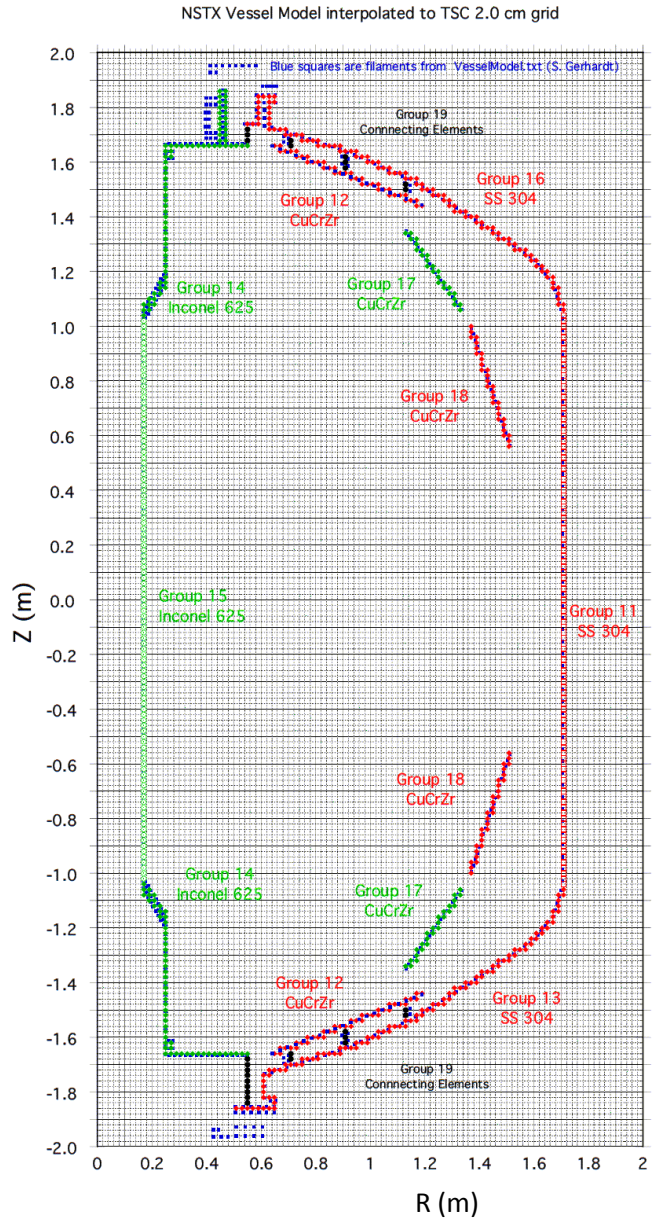
$$\mathbf{v} \equiv \mathbf{v}_i - \mathbf{v}_i^* = \mathbf{v}_e - \mathbf{v}_e^* + \frac{\mathbf{J}_\parallel}{ne}$$

Artificial sound wave model for κ_\parallel :

$$\frac{\partial T}{\partial t} = s \frac{\mathbf{B} \cdot \nabla u}{\rho}$$

$$\frac{\partial u}{\partial t} = s \mathbf{B} \cdot \nabla T + \nu \nabla^2 u$$

Meshing the NSTX Vessel



Toroidally Asymmetric Halo Current Figures of Merit

Toroidal peaking factor (TPF): If there are N poloidal planes, $j=1,2,3,\dots,N$, then

$$TPF \equiv \frac{\text{Max}_{j=1}^N \left\{ \oint_{\Gamma_j} R |\mathbf{J} \cdot \hat{n}| dl \right\}}{\frac{1}{N} \sum_{j=1}^N \left\{ \oint_{\Gamma_j} R |\mathbf{J} \cdot \hat{n}| dl \right\}}$$

Halo fraction (HF):

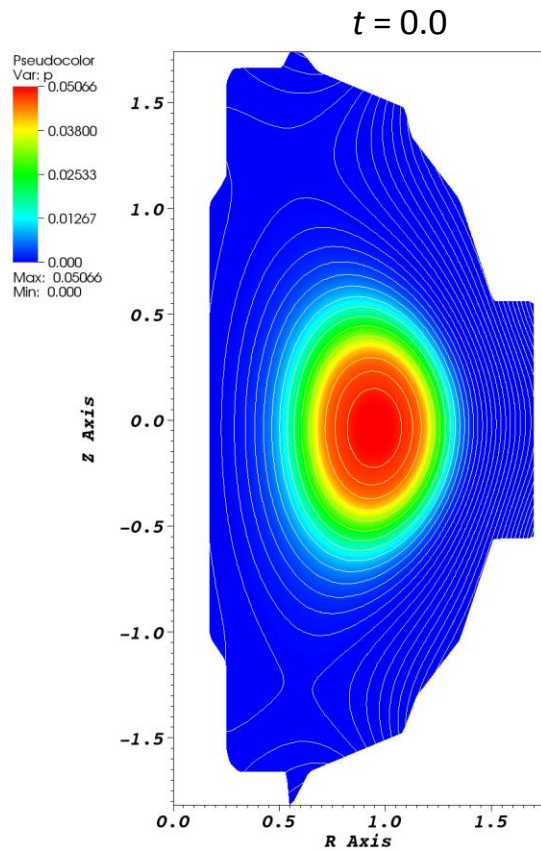
$$HF \equiv \frac{\frac{2\pi}{N} \sum_{j=1}^N \left\{ \oint_{\Gamma_j} R |\mathbf{J} \cdot \hat{n}| dl \right\}}{I_{p0}},$$

where I_{p0} is the total plasma current in the initial equilibrium.

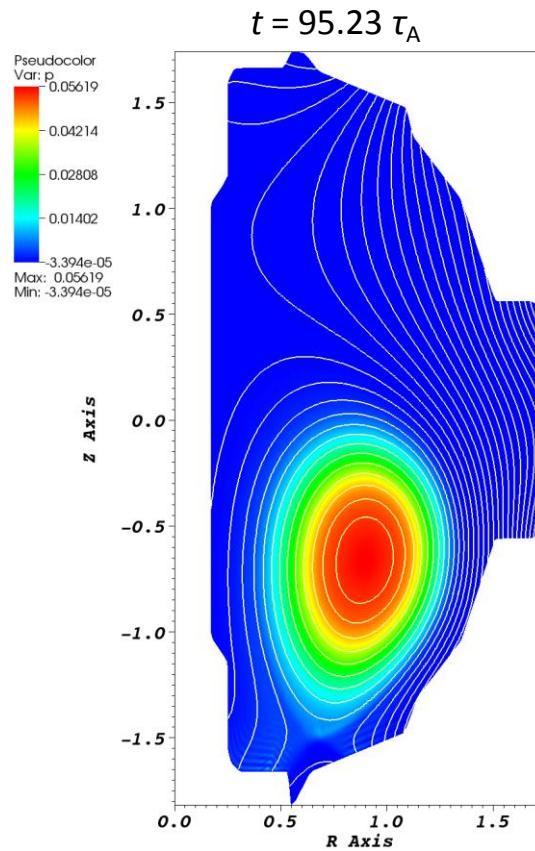
Low-plasma-resistivity simulation parameters

| | |
|---|------------------------------|
| Plasma resistivity on axis* $\eta_0=S^{-1}$ | 5×10^{-6} |
| $\eta_{\text{vacuum}} / \eta_0$ | 12000 |
| $\eta_{\text{wall}} / \eta_0$ | 10000 ($\tau_w/\tau_A=20$) |
| Prandtl number μ / η_0 | 20 |
| Perpendicular heat conduction κ_{\perp} / η_0 | 2 |
| Effective parallel heat conduction v_{Te} / v_A | 2 |
| Density evolution | Off (uniform, constant) |
| Size of initial $n=1$ perturbation | 5×10^{-3} |
| Number of toroidal modes | 5 (16 poloidal planes) |

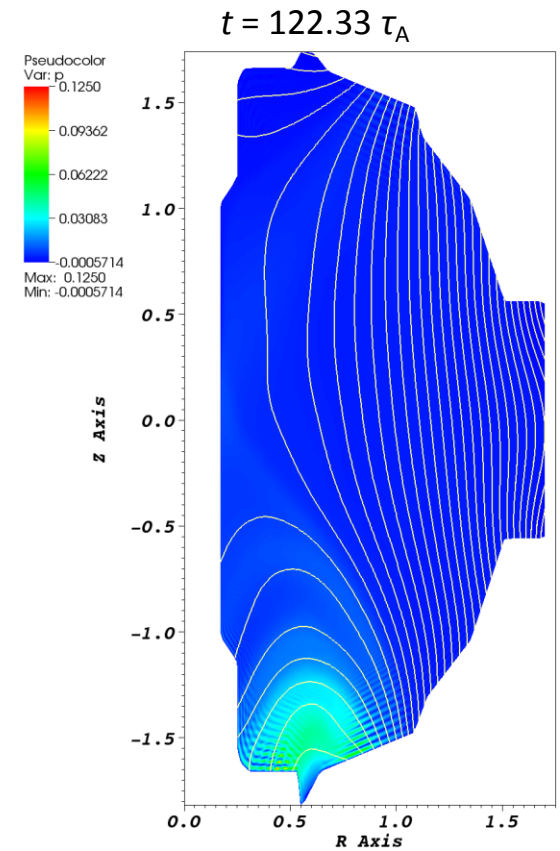
Low-resistivity Snapshots



Initial VDE-unstable equilibrium
 $q_0 \approx 1$

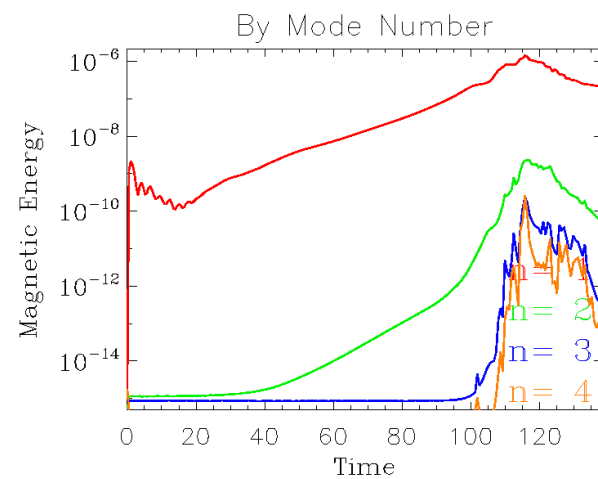
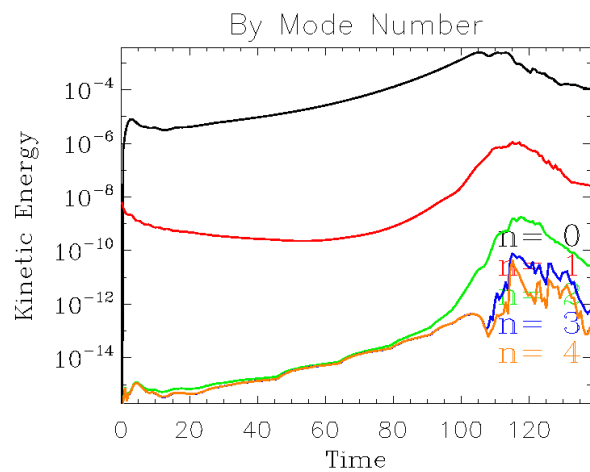
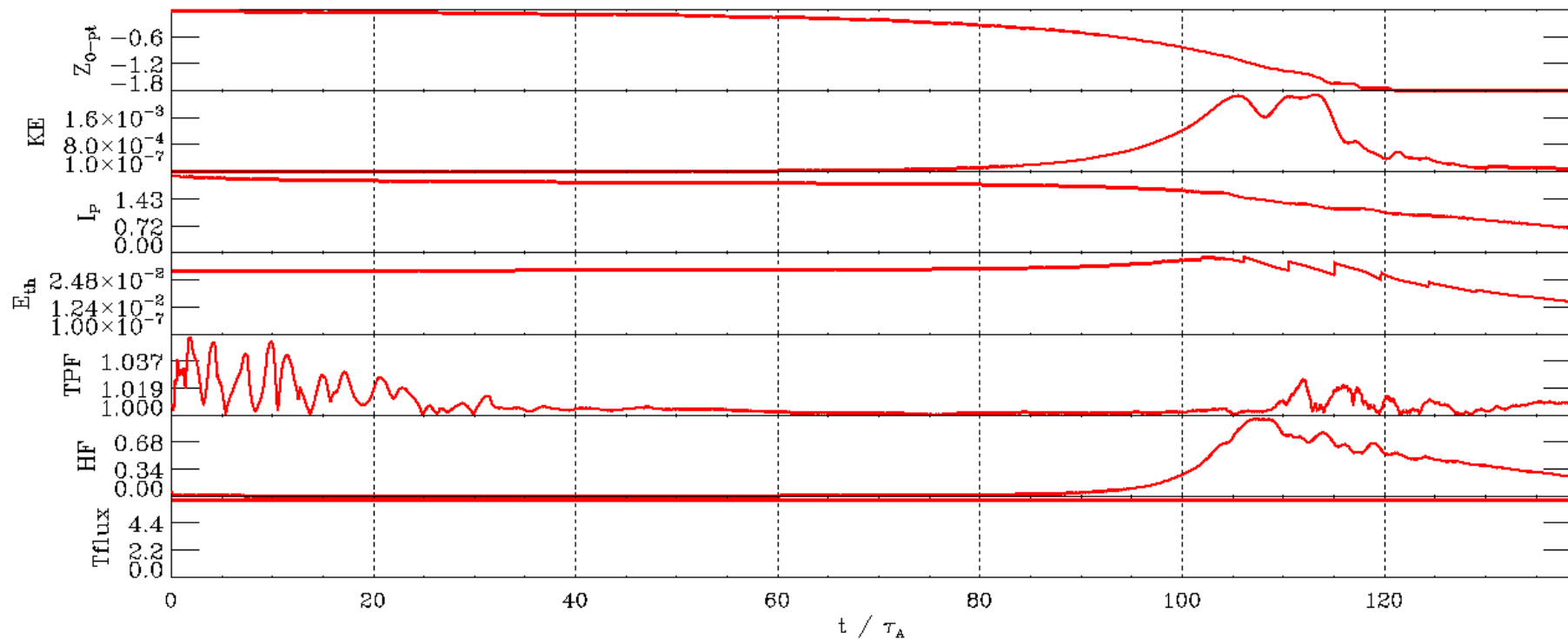


Plasma is displaced downward,
 $n=1$ instability is not in
evidence.



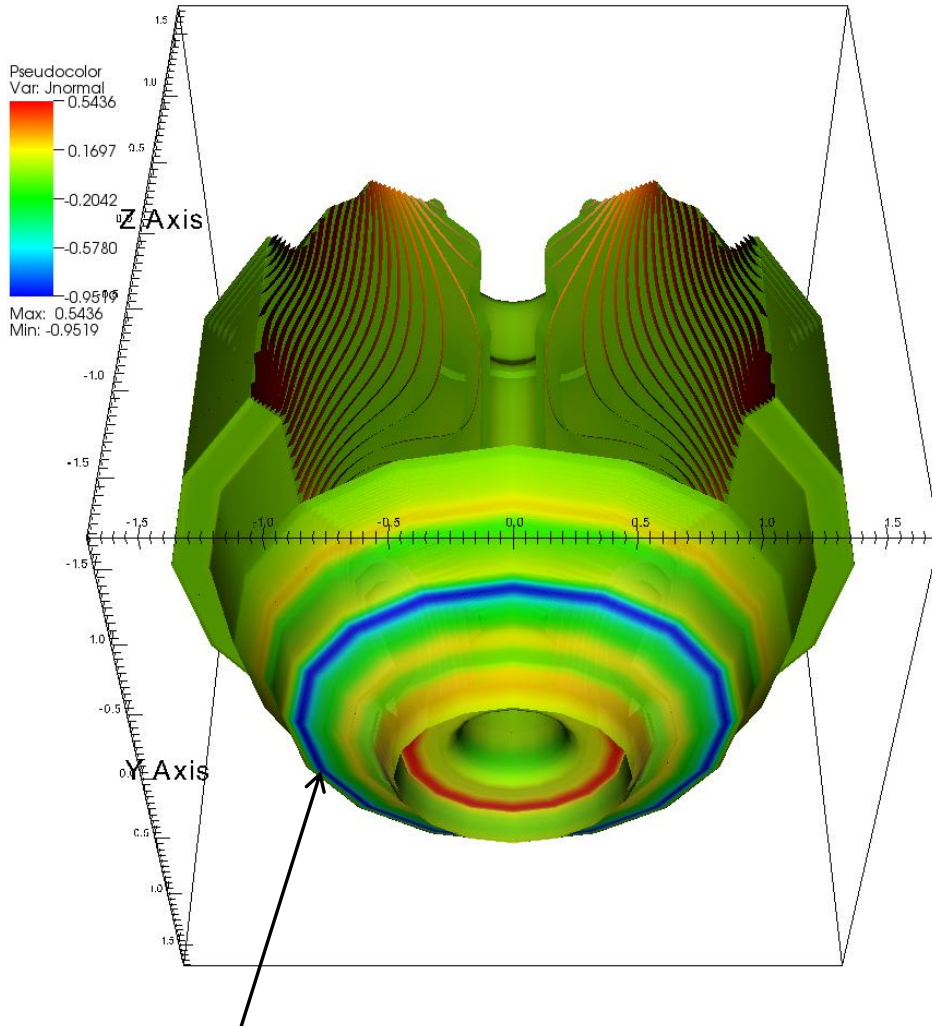
Confinement is lost, heat
deposited in divertor region.

Time History

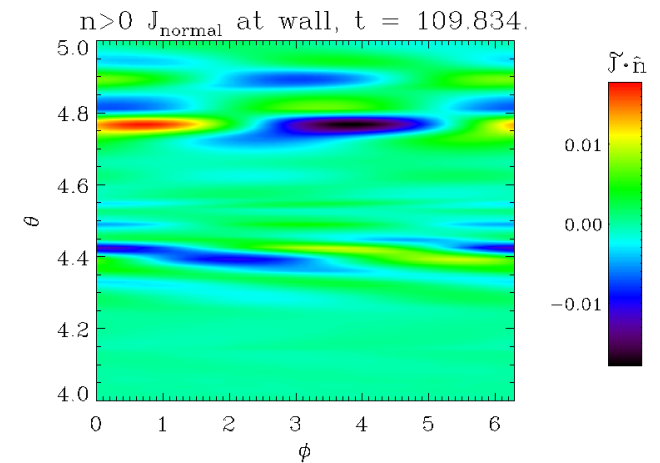
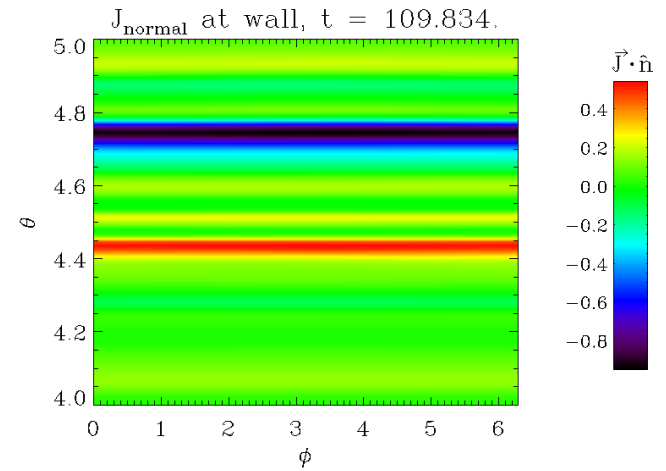


Halo Current Distribution at Peak

$t = 109.834$



Current peaks on lower Group 12 plate.

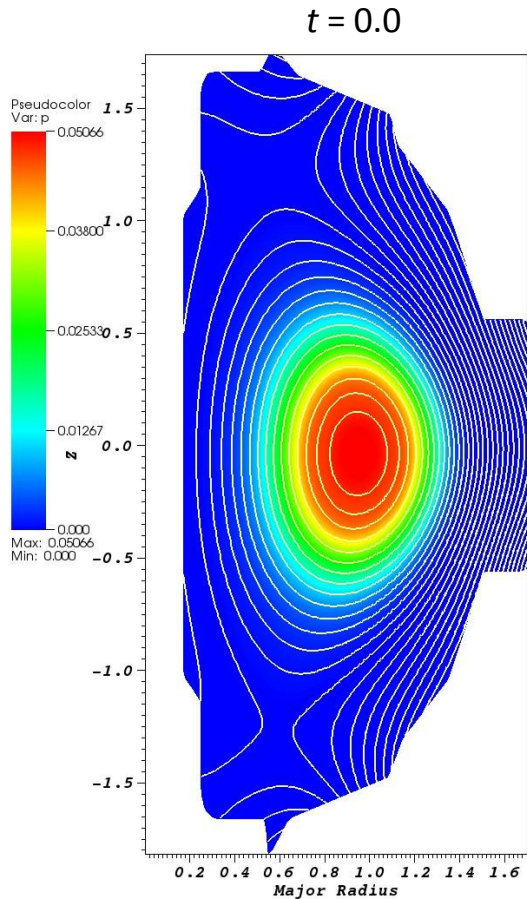


$n=1$ component is much smaller than $n=0$.

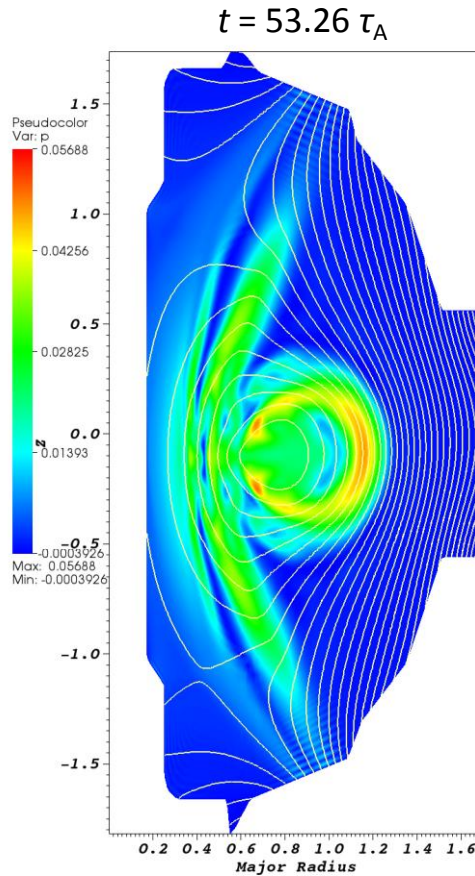
High-plasma-resistivity parameters

| | |
|---|----------------------------|
| Plasma resistivity on axis* $\eta_0=S^{-1}$ | 5×10^{-4} |
| $\eta_{\text{vacuum}} / \eta_0$ | 120 |
| $\eta_{\text{wall}} / \eta_0$ | 100 ($\tau_w/\tau_A=20$) |
| Prandtl number μ / η_0 | 0.2 |
| Perpendicular heat conduction κ_{\perp} / η_0 | 0.02 |
| Effective parallel heat conduction v_{Te} / v_A | 2 |
| Density evolution | Off (uniform, constant) |
| Size of initial $n=1$ perturbation | 5×10^{-3} |
| Number of toroidal modes | 5 (16 poloidal planes) |

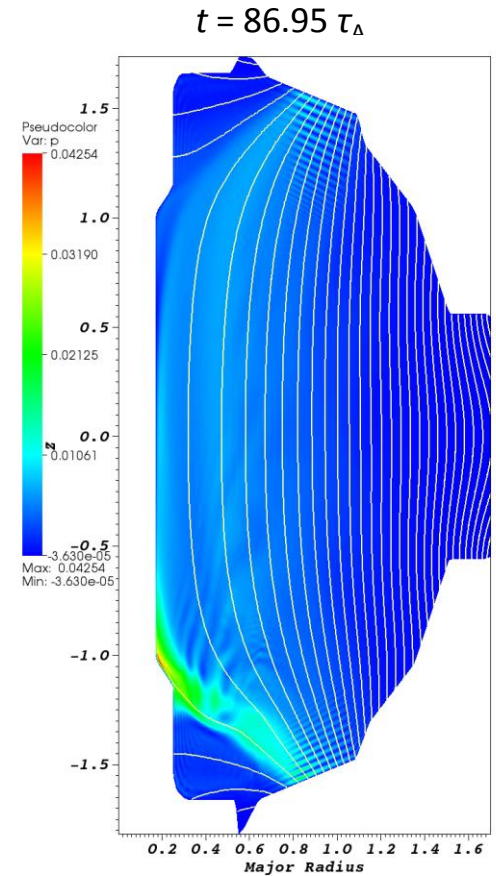
High-resistivity Snapshots



Initial VDE-unstable equilibrium

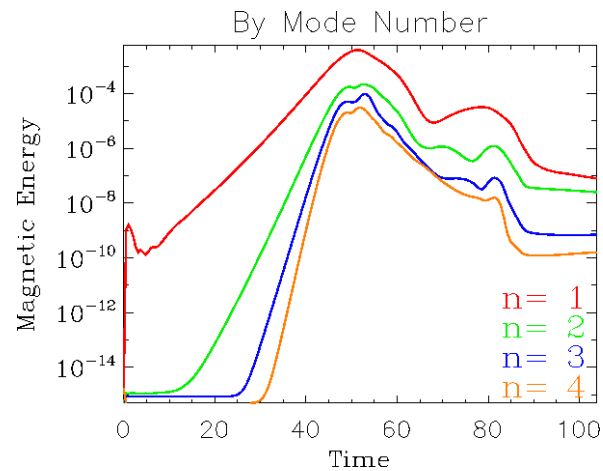
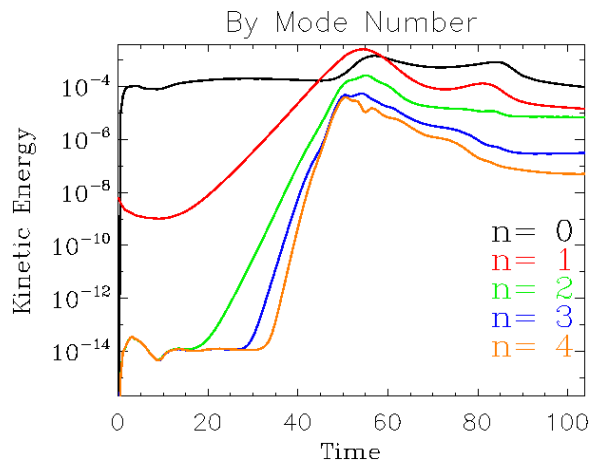
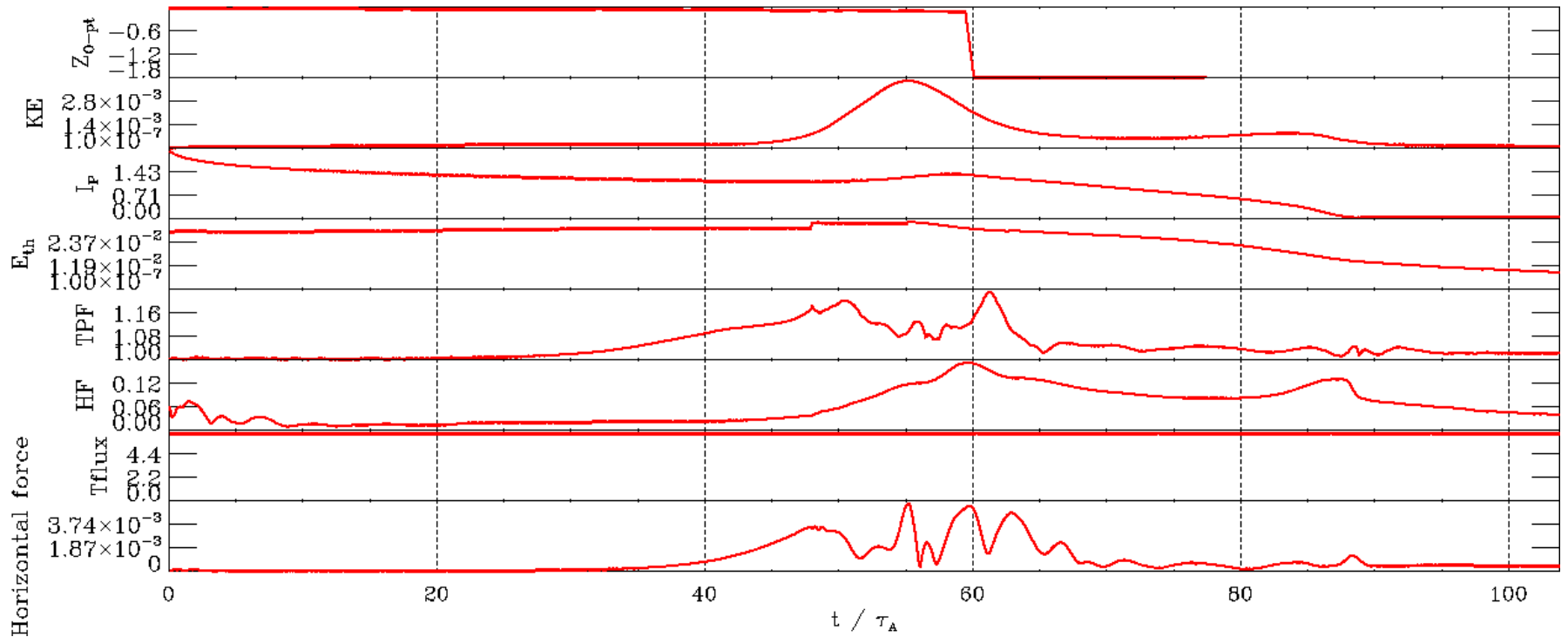


Higher- n instabilities disperse heat before significant vertical displacement occurs.



Confinement is lost rapidly; heat deposited on inboard wall.

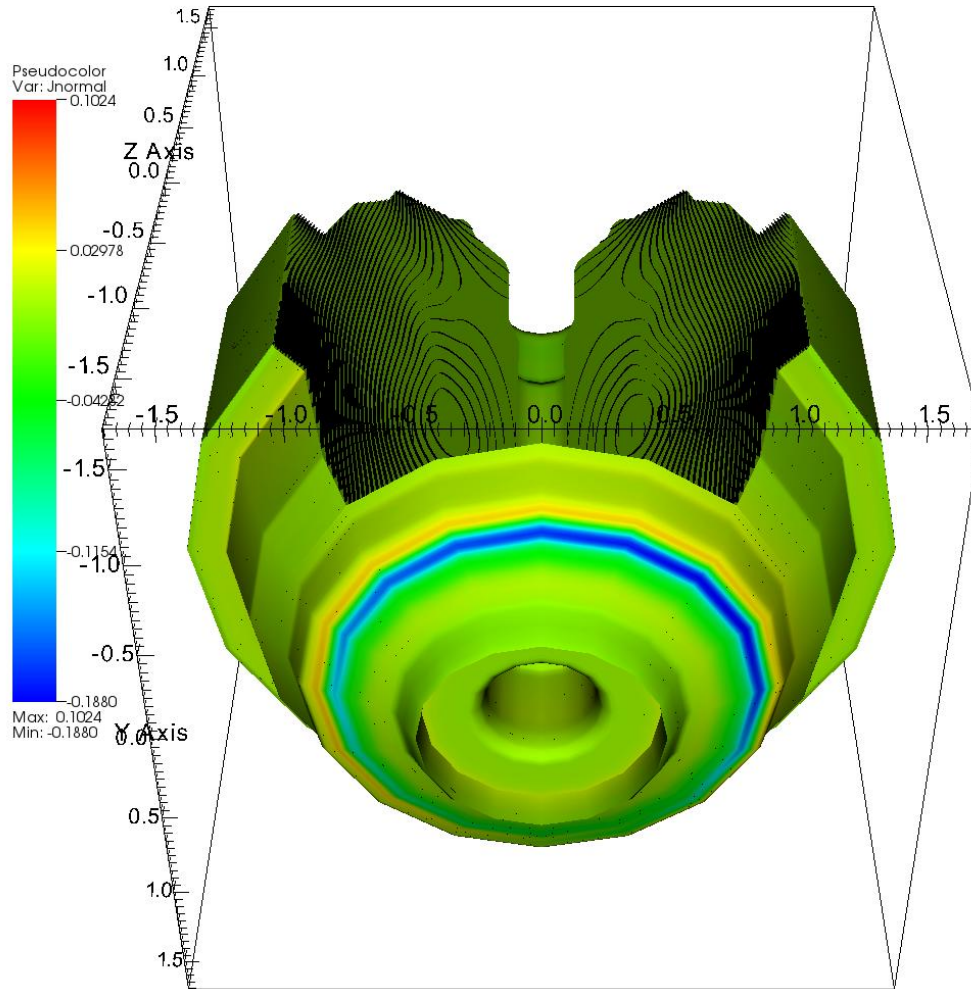
Time History



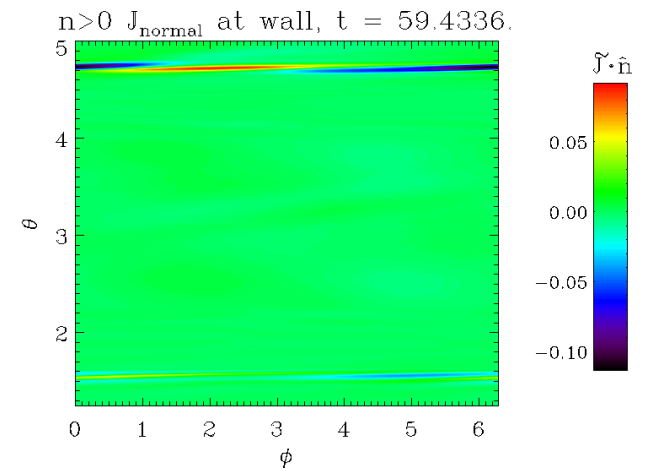
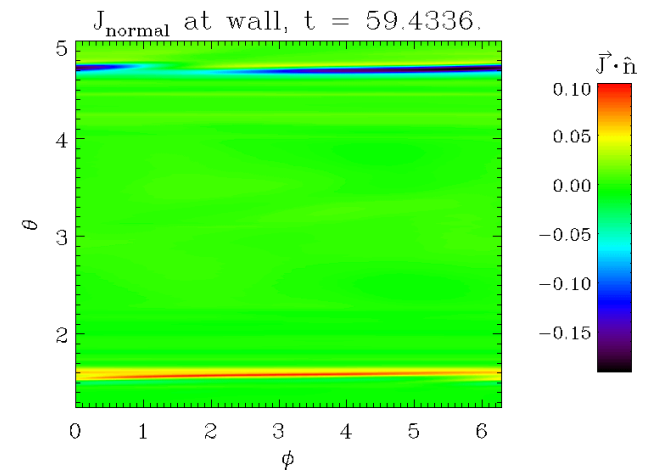
At $t=24.88$, $q=1$ surface is at $s=0.59$; $q_{min} \approx 0.927$.

Halo Current Distribution at Peak

$t = 59.434$



Current peaks on lower Group 12 plate.



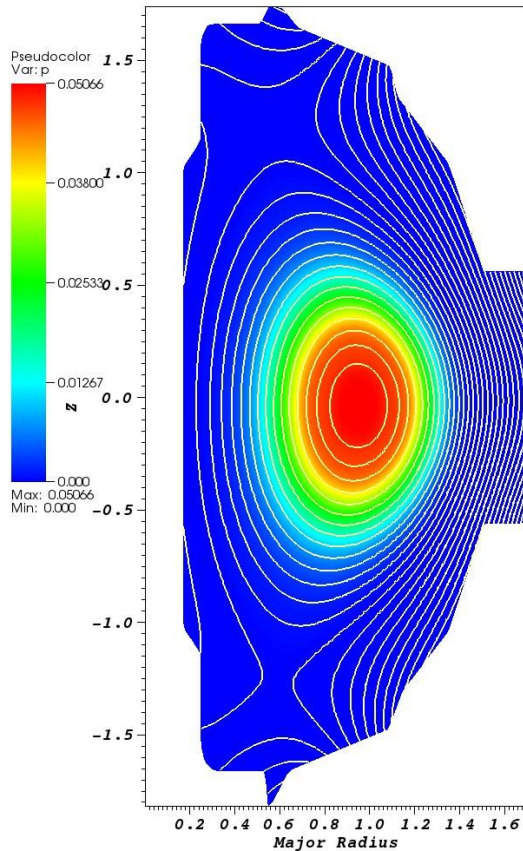
$n=1$ component is about half as large as $n=0$.

Worst-case scenario for sideways force: intermediate resistivity

| | |
|---|-----------------------------|
| Plasma resistivity on axis* $\eta_0=S^{-1}$ | 2×10^{-5} |
| $\eta_{\text{vacuum}} / \eta_0$ | 3000 |
| $\eta_{\text{wall}} / \eta_0$ | 2500 ($\tau_w/\tau_A=20$) |
| Prandtl number μ / η_0 | 5 |
| Perpendicular heat conduction κ_{\perp} / η_0 | 0.5 |
| Effective parallel heat conduction v_{Te} / v_A | 2 |
| Density evolution | Off (uniform, constant) |
| Size of initial $n=1$ perturbation | 5×10^{-3} |
| Number of toroidal modes | 5 (16 poloidal planes) |

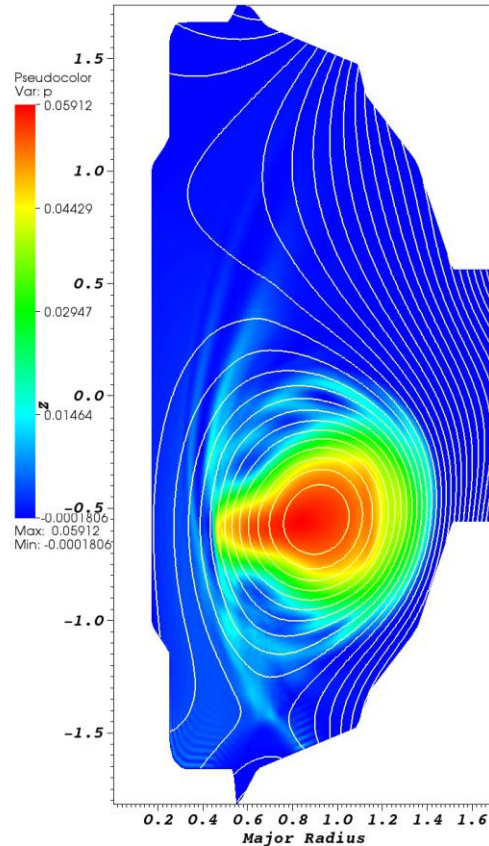
Snapshots

$t = 0.0$



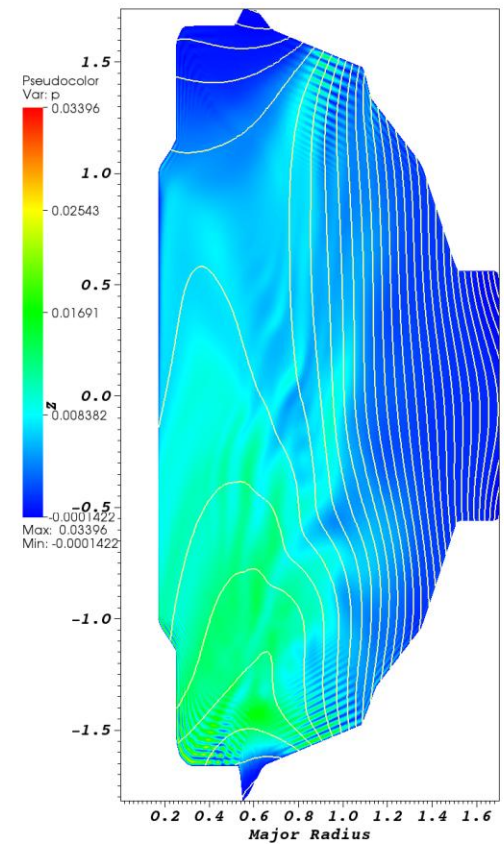
Initial VDE-unstable equilibrium

$t = 106.81 \tau_A$



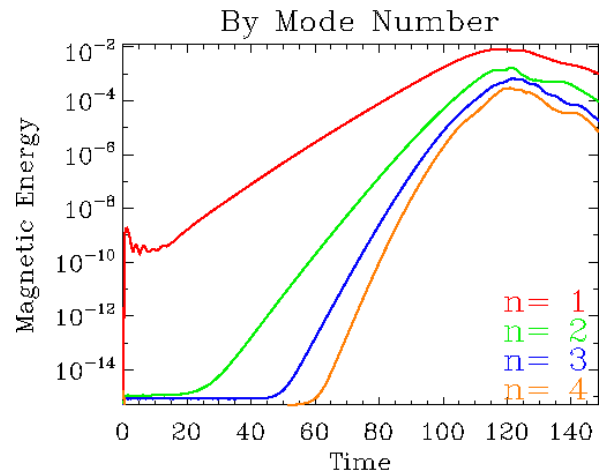
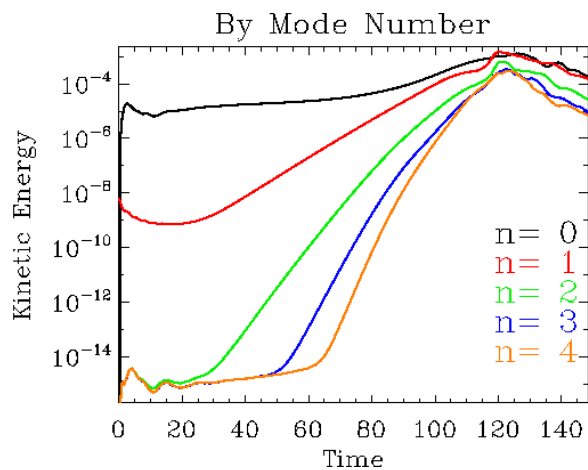
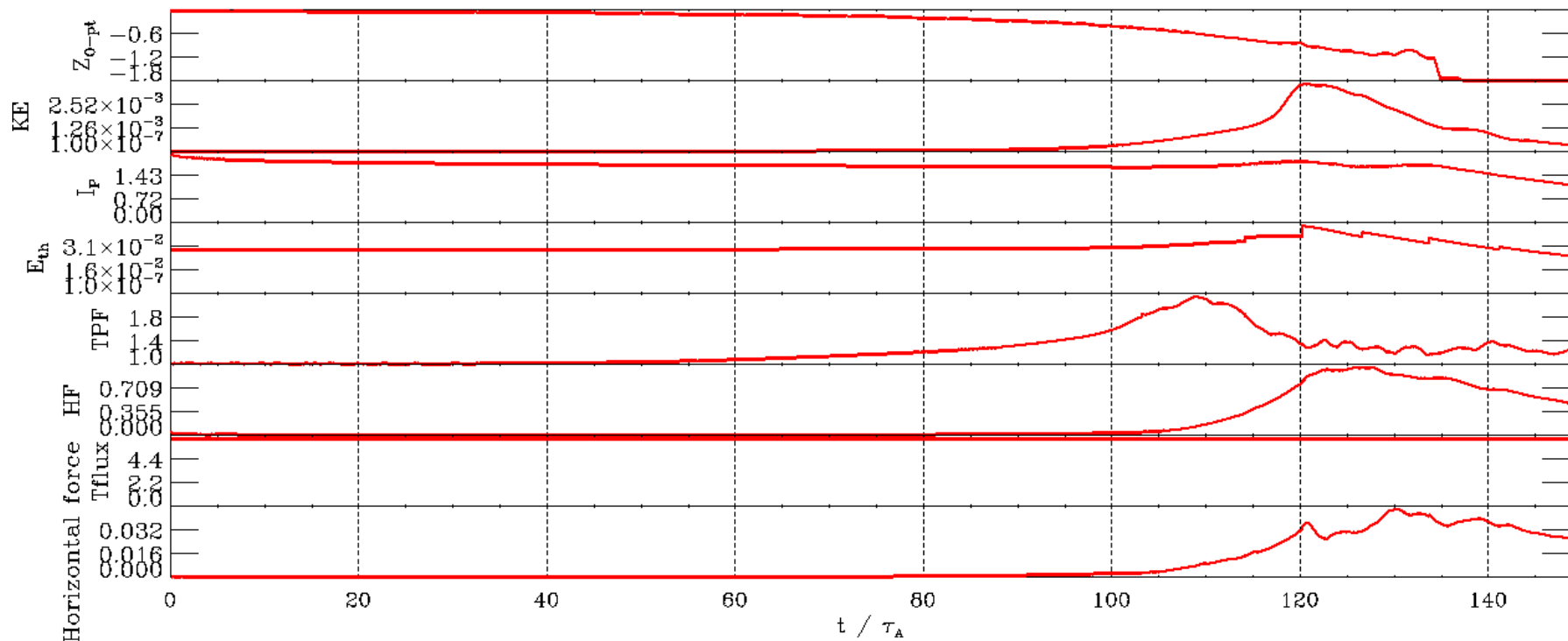
$n=1$ instability is concurrent with energetic stage of vertical displacement event.

$t = 148.68 \tau_A$



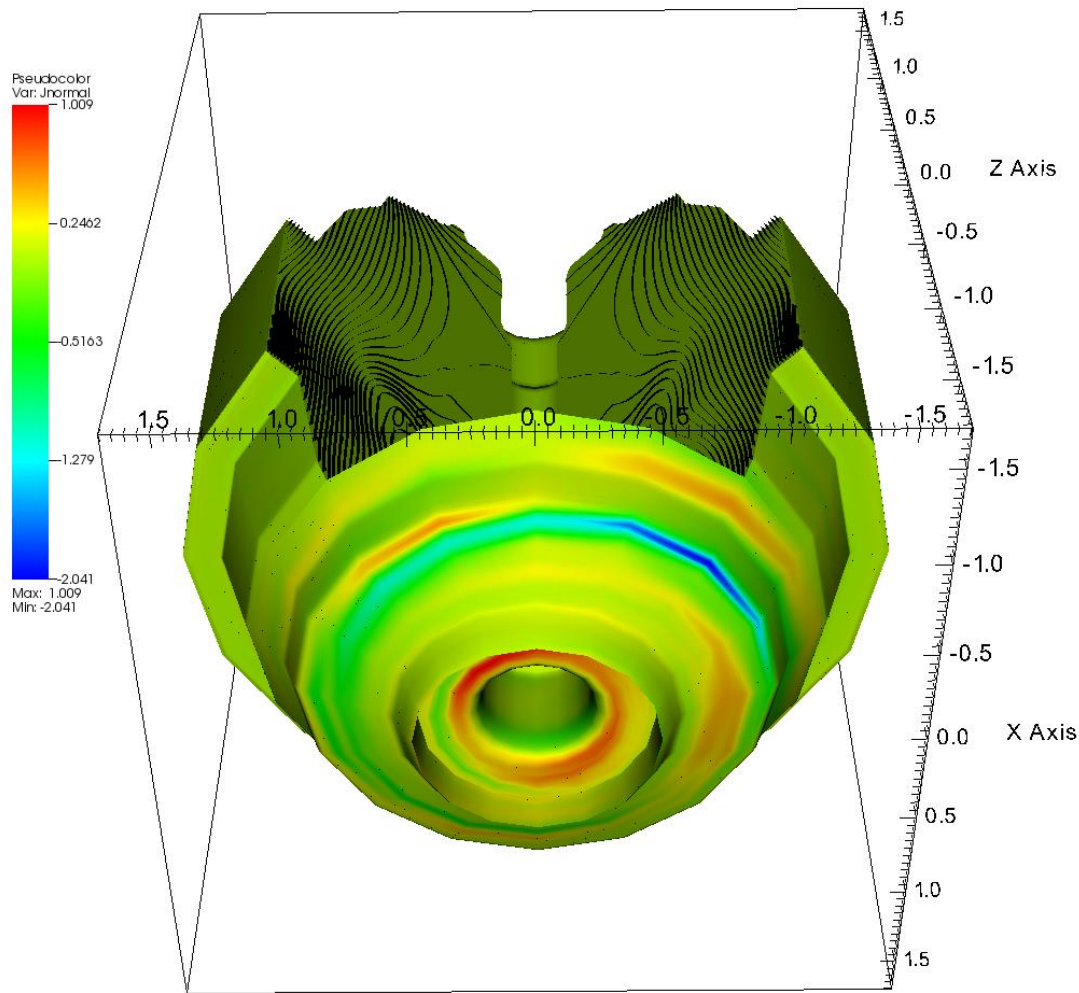
Confinement is lost, heat deposited in divertor region.

Time History



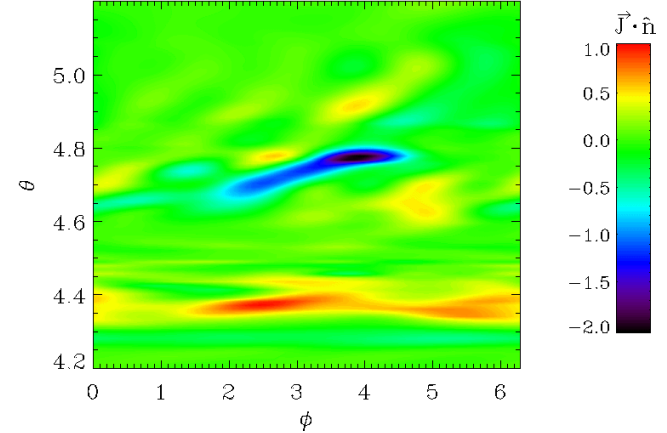
Halo Current Distribution at Peak

$t = 122.854$

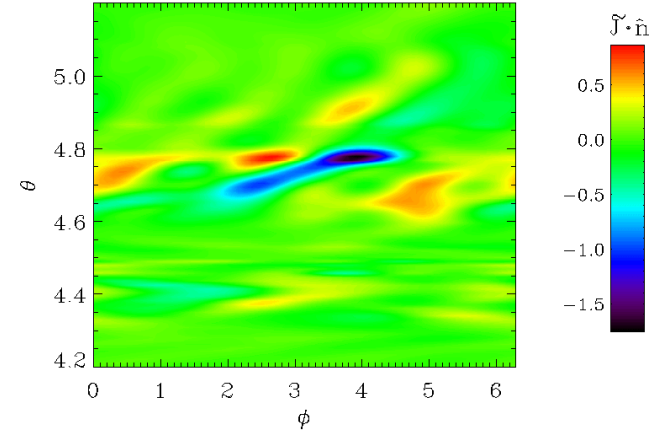


Current peaks on lower Group 14 wall.

J_{normal} at wall, $t = 122.854$.

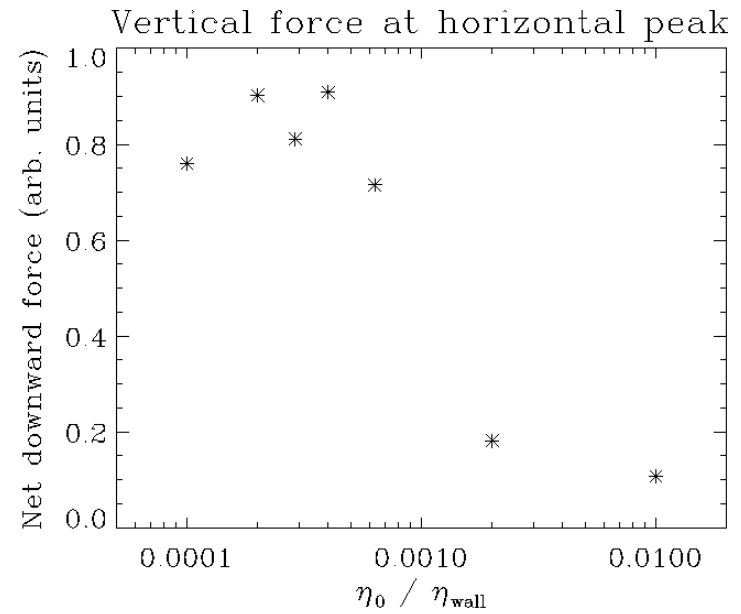
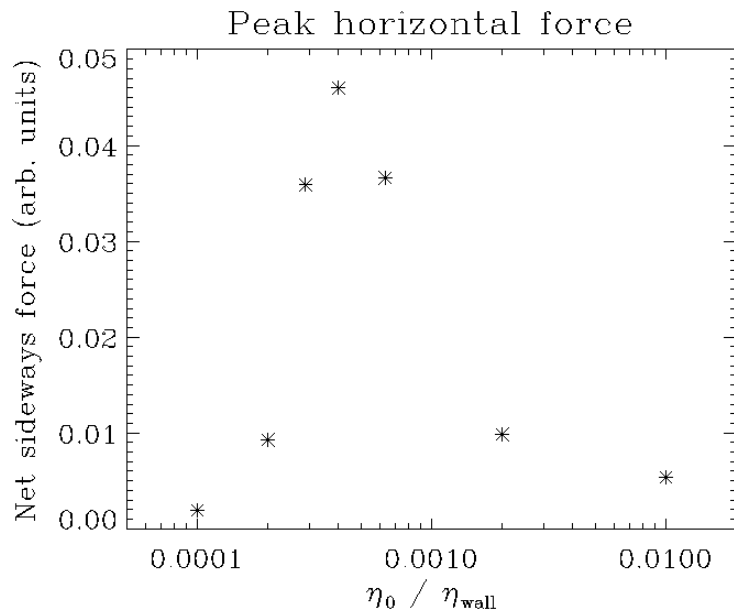
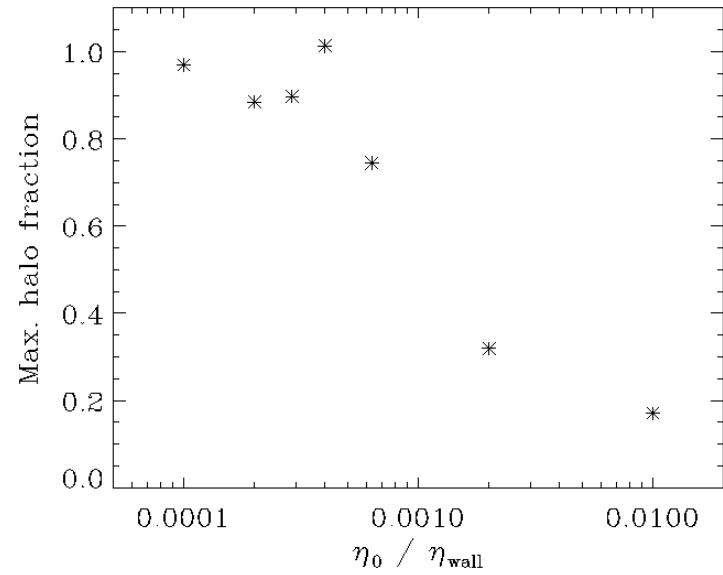
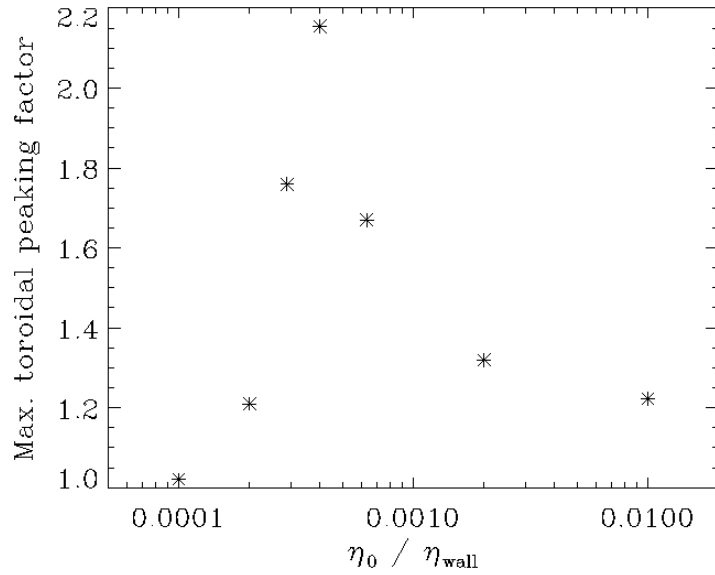


$n > 0$ J_{normal} at wall, $t = 122.854$.

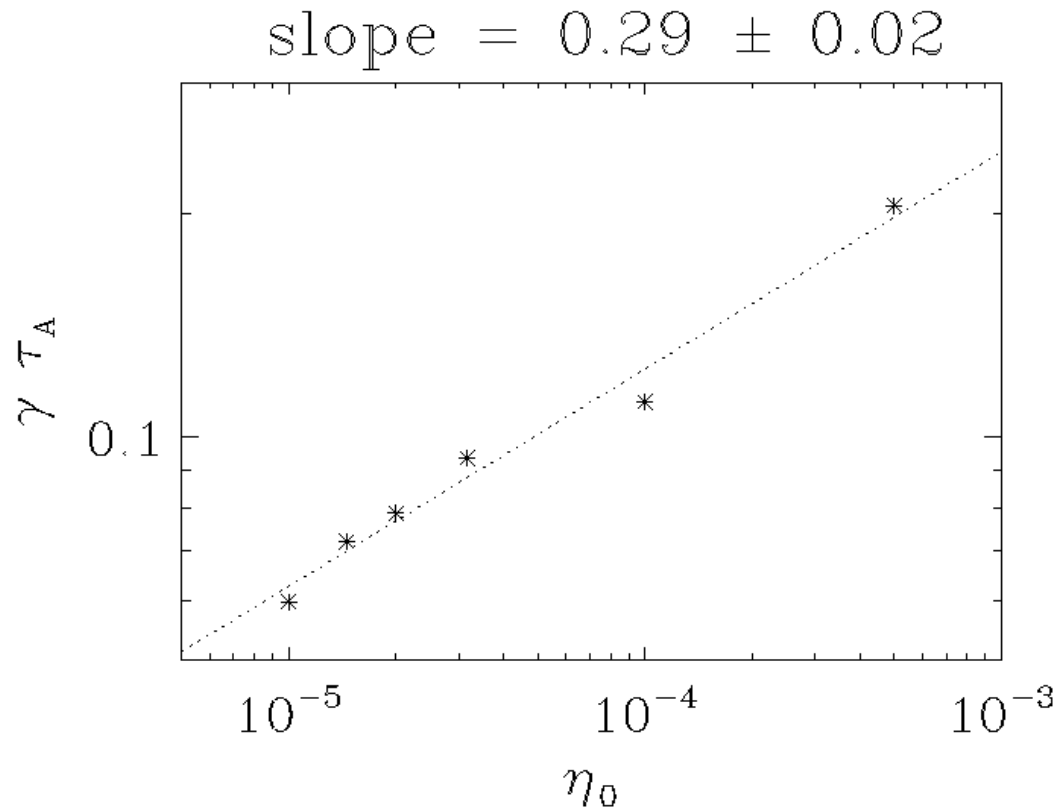


$n=1$ component almost as large as $n=0$.

Resistivity Scaling Results



$n=1$ mode appears to be resistive



Actual plasma has $\eta_{\text{wall}} \gg \eta_0$, so the observed MHD mode is likely ideal and destabilized by scrape-off of high- q surfaces during VDE.

Conclusions

- When plasma resistivity is large compared to wall resistivity ($\eta_0/\eta_{\text{wall}} > 10^{-3}$), the $n=1$ instability occurs before the VDE begins. This instability is very energetic, but dissipates heat before the plasma contacts the wall, resulting in relatively low disruption halo currents and forces.
- When plasma resistivity is small compared to wall resistivity ($\eta_0/\eta_{\text{wall}} < 10^{-4}$), the VDE is completed before the $n=1$ mode is destabilized. This results in higher divertor heat flux and halo fraction (since the thermal and current quenches have not occurred before the plasma makes contact), but very low toroidal peaking factor and net sideways force (since the plasma remains essentially axisymmetric throughout the disruption).
- When plasma resistivity is such that the $n=1$ and $n=0$ modes are destabilized on the same time scale, the plasma that hits the wall is non-axisymmetric but still very energetic, resulting in much higher TPF and sideways forces and somewhat elevated halo fraction and vertical force.
- In all cases, the vertical force on the vessel is greater than the net horizontal force by more than an order of magnitude.

Future Work

- The wall time for the cases shown here is unrealistically small (τ_{wall} for NSTX is estimated to be roughly 10 ms). Simulations with wall times up to $4000 \tau_A$ have been carried out, but Spitzer resistivity profiles result in rippling modes that destroy confinement before the VDE has begun.
- Density evolution can alter the dynamics but has been omitted thus far because of problems with numerical stability.
- Therefore, ongoing work involves running with a more ideal plasma and attempting to stabilize the rippling mode and improve the numerics in the presence of a density gradient.
- Quantitative validation against NSTX observations remains to be done.